

Large Deflection of Thin Plates in Convex or Concave Cylindrical Bending

Vivek A. Jairazbhoy¹; Pavel Petukhov²; and Jianmin Qu, M.ASCE³

Abstract: Considered in this paper is a special case relating to the large deflection of a thin beam. One end of the beam is fixed (i.e., clamped) to a rigid wall, whereas the other end is placed on a flat surface of arbitrary orientation. In previous studies, unique and non-unique solutions to the deflected shape were derived for cases in which the curvature of the beam experiences at least one change in sign. In this paper, a special case is examined in which the curvature of the beam does not change sign. Experimental results from photographs of deflected beams are presented to support the numerical predictions. An excellent agreement was found between the photographed and the predicted shapes. DOI: [10.1061/\(ASCE\)EM.1943-7889.0000321](https://doi.org/10.1061/(ASCE)EM.1943-7889.0000321). © 2012 American Society of Civil Engineers.

CE Database subject headings: Deflection; Plates; Beams; Bending.

Author keywords: Large deflection; Plates; Beams; Bending.

Introduction

This paper deals with the bending of thin plates (i.e., beams) into shapes that involve large deflections. In an earlier work (Jairazbhoy et al. 2008; Xue et al. 2003), unique and non-unique solutions to the deflected shape are derived for cases in which the curvature of the beam experiences at least one change in sign. This paper analyzes the shapes for which the curvature of the beam does not change in sign. The authors of this paper defined such a beam as “concave” if the slope of the beam (i.e., the angle between the local tangent to the beam and the x -axis) decreased monotonically along the length of the beam from the point of fixture. The authors defined the beam as “convex” if the slope of the beam conversely increased monotonically along the length of the beam from the point of fixture.

The problem of bending thin plates into various controlled shapes occurs frequently in a number of emerging technical areas such as optical fiber packaging and the packaging of flexible circuits (Freitag et al. 2000; Isaak and Uka 2000). In many instances, the shape and the accompanying pre-stressed state must be captured to package the beam and to anticipate its response to vibration while in operation (Cornil et al. 2007). Jairazbhoy et al. (2008) discuss several packaging applications that require an understanding of how beams behave in cylindrical bending. In many such applications, the deformation can be analyzed by using thin plate (or beam) theories.

¹General Motors Company, VEC Buildings 4AY25A, 30001 Van Dyke, Bldgs. 2-10, P.O. Box 9020, Warren, MI 48090-9020; formerly, Ford Motor Company, 2H-F70 PDC, 20901 Oakwood Blvd, Dearborn, MI 48124 (corresponding author). E-mail: jairazbhoy@sbcglobal.net

²Visteon Corporation, One Village Center Drive, 40-3-097, Van Buren Township, MI 48111.

³Dept. of Civil and Environmental Engineering, Northwestern Univ., Evanston, IL 60208.

Note. This manuscript was submitted on October 9, 2009; approved on August 1, 2011; published online on August 3, 2011. Discussion period open until July 1, 2012; separate discussions must be submitted for individual papers. This technical note is part of the *Journal of Engineering Mechanics*, Vol. 138, No. 2, February 1, 2012. ©ASCE, ISSN 0733-9399/2012/2-230-234/\$25.00.

Governing Equations

Jairazbhoy et al. (2008) and Xue et al. (2003) developed the governing equations for the large cylindrical deflection of a thin beam. These equations form the basis for the analysis presented in this paper. For cylindrical deformation, the boundary conditions and loads vary only in two directions. The field quantities (e.g., deflections, stress, strain) consequently vary in two dimensions. One end of the beam is fixed (i.e., clamped) to a rigid wall, whereas the other end (i.e., the free end) is placed on a flat surface of arbitrary orientation. Fig. 1 depicts a 2-dimensional (2-D) cantilever beam of length L with a prescribed displacement (x_A, y_A) and rotation angle (θ_f) at the free end. Under certain assumptions, Jairazbhoy et al. (2008) derived the following equation for the variation of the local rotation angle θ of the beam along its length coordinate S :

$$EI \frac{d^2\theta}{dS^2} = -T \cos(\theta - \theta_f) + F_A \sin(\theta - \theta_f), \quad (1)$$

where EI is the bending rigidity of the beam, and T and F_A are the components of the concentrated force on the free end that is perpendicular to and tangent to, respectively, the fastening surface. Both T and F_A are unknown and must be solved as part of the boundary value problem.

Eq. (1) is derived by substituting Hooke's law for linear elastic materials into equilibrium relationships for the beam (subject to certain assumptions) and presenting the resulting relationship in a manner that describes the evolution of the rotation angle along the length of the beam. Xue et al. (2003) presented a semi-analytical solution for the special case of $F_A = 0$. Jairazbhoy et al. (2008) presented solutions for a significant subset of the solution space in which the curvature of the beam vanishes for at least one value of the rotation angle θ lying between $-\pi$ and π ; this permits a smooth change of sign of the curvature at that value of θ .

Beam with Either a Positive or Negative Curvature for All θ

In this section, the authors examine the portion of the solution space in which the curvature is either positive or negative for all θ . For

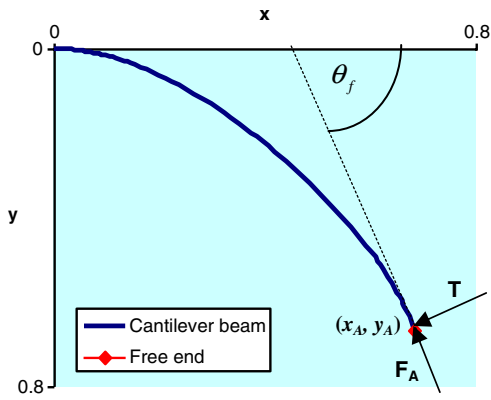


Fig. 1. Cantilever beam with a prescribed displacement and rotation angle

$$\frac{d\theta}{dS} \neq 0,$$

the left-hand side of Eq. (1) may be rewritten by using the following relationship:

$$\frac{d^2\theta}{dS^2} = \frac{d}{dS} \left(\frac{d\theta}{dS} \right) = \frac{d}{d\theta} \left[\frac{1}{2} \left(\frac{d\theta}{dS} \right)^2 \right]. \quad (2)$$

Integrating with respect to θ yields

$$\frac{1}{2} \left(\frac{d\theta}{dS} \right)^2 = -\frac{T}{EI} \sin(\theta - \theta_f) - \frac{F_A}{EI} \cos(\theta - \theta_f) + C_0. \quad (3)$$

Eq. (3) effectively expresses the curvature of the beam as a function of the rotation angle, in terms of three unknowns: T , F_A , and the integration constant C_0 . Rearranging the equation yields

$$\frac{Ld\theta}{dS} = \pm \sqrt{2[C - \bar{T} \sin(\theta - \theta_f) - \bar{F}_A \cos(\theta - \theta_f)]}, \quad (4)$$

where C is a constant,

$$\bar{T} = \frac{TL^2}{EI}, \quad (5)$$

and

$$\bar{F}_A = \frac{F_AL^2}{EI}. \quad (6)$$

The sign of the square root on the right-hand side of Eq. (4) is determined by the curvature of the beam, and is apparent from the coordinates of the free end of the beam. Separating the variables θ and S in Eq. (3) and integrating over the length of the beam yields an integral relationship among the three unknowns T , F_A , and C , in terms of the length of the beam, L , as follows:

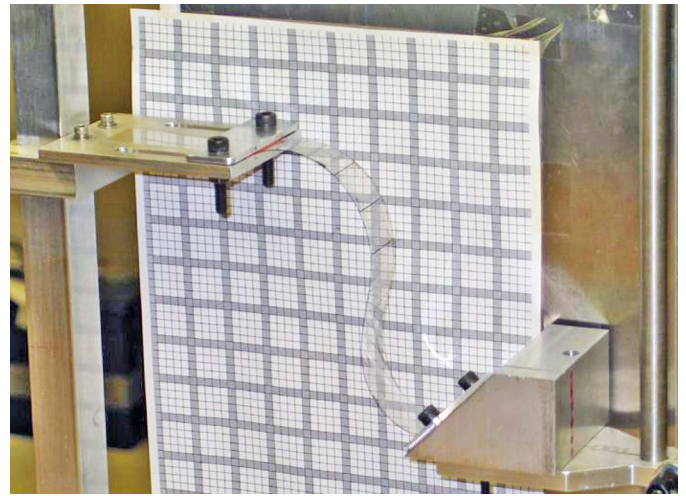


Fig. 2. Experimental setup

$$\int_0^L dS = \pm \int_{\theta} \frac{Ld\theta}{\sqrt{2[C - \bar{T} \sin(\theta - \theta_f) - \bar{F}_A \cos(\theta - \theta_f)]}} = L. \quad (7)$$

To obtain the deformed configuration of the beam, it is necessary to calculate the coordinates x and y of the deflection curve as functions of S . For a beam with zero axial extension, these coordinates may be expressed as follows:

$$dx = \cos \theta dS; \quad dy = \sin \theta dS. \quad (8)$$

On the basis of Eqs. (4) and (8), the prescribed displacements at the free end of the beam can be enforced by integrating the coordinates x and y over the length of the beam, as follows:

$$\int_0^{x(L)} dx = \pm \int_{\theta} \frac{L \cos \theta d\theta}{\sqrt{2[C - \bar{T} \sin(\theta - \theta_f) - \bar{F}_A \cos(\theta - \theta_f)]}} = x_A \quad (9)$$

$$\int_0^{y(L)} dy = \pm \int_{\theta} \frac{L \sin \theta d\theta}{\sqrt{2[C - \bar{T} \sin(\theta - \theta_f) - \bar{F}_A \cos(\theta - \theta_f)]}} = y_A \quad (10)$$

In Eqs. (7), (9), and (10), the integrands are never singular when the following relationship holds for all θ in the range $(0, \theta_f)$:

$$C > \bar{T} \sin(\theta - \theta_f) + \bar{F}_A \cos(\theta - \theta_f) \quad (11)$$

Table 1. Analytical Results

Case number	Input				Output			
	\bar{x}_A	\bar{y}_A	θ_f (deg)	L	\bar{T}	\bar{F}_A	C	% error
1	0.675	0.703	86.0	219.1	-74.2	91.0	234.8	2.7
2	0.632	0.686	86.0	236.1	-14.5	20.0	49.9	3.1
3	0.662	0.640	75.6	218.4	1.6	-0.3	-0.1	4.2
4	0.680	0.657	75.6	212.6	-4.5	10.3	23.1	3.3
5	0.692	0.669	75.6	208.9	-14.0	26.0	59.3	3.9

If this is true along the entire length of the beam, then the beam curvature does not change sign (i.e., no “points of inflection” exist). Therefore, θ changes monotonically with S , and the limits of integration in Eqs. (7), (9), and (10) are $(0, \theta_f)$. Jairazbhoy et al. (2008) refer to solutions that exhibit no points of inflection as “Type 1” (e.g., Fig. 1). Their formulation is intended to capture Type 1 solutions that exhibit no points of inflection for θ lying in the range $(0, \theta_f)$, but do exhibit points of inflection for at most two values of θ outside the range $(0, \theta_f)$. The formulation in this paper is intended to capture Type 1 solutions that exhibit no points of inflection for θ lying in the range $(0, \theta_f)$, regardless of the behavior outside the range $(0, \theta_f)$.

Given the length L and the coordinates of the free end of the beam x_A and y_A , Eqs. (7), (9), and (10) are solved iteratively for the three unknowns T , F_A , and C . The quadrature is carried out by the trapezoidal rule. If given T , F_A , and C , then the quantities S , x , and y (which represent the axial coordinate and the Cartesian coordinates along the beam) can be calculated for incremental values of θ .

Results and Discussion

Fig. 2 shows the experimental setup used to photograph a flexible beam that was fastened to produce a variety of relevant beam shapes. The material of the beam is polyethylene terephthalate

(PET). Jairazbhoy et al. (2008) used the same setup to produce beam shapes. The beam is fastened at both ends by adjustable clamps. The motion of the fastened ends in a plane parallel to the desired mid-plane of the beam is used to establish the distance and angle between the fasteners (i.e., to establish the prescribed displacement $[x_A, y_A]$ of the free end). The length of the beam is varied by clamping down at different locations along the beam. At the free end, the beam is fastened at an angle to the horizontal, thus establishing the rotation angle (θ_f). A digital camera photographed the shape of the beam. The leading edge of the beam is highlighted to aid the visual comparison of the photographed shapes against the analytical predictions.

Fig. 1 shows that if the tangent to the free end of the beam intersects the positive x -axis, then a beam shape with no points of inflection is always possible by choosing a small enough length of the beam. If conversely the tangent to the free end of the beam intersects the negative x -axis, then a beam shape with no points of inflection is impossible, regardless of the length of the beam. The experimental cases in this study are selected by picking the location of the free end and the rotation angle of the beam so that the tangent to the free end of the beam intersects the positive x -axis, thereby ensuring the existence of a beam shape with no points of inflection. Starting from a beam length that is large enough to produce at least one point of inflection, the length is reduced until a suitable shape with no points of inflection is attained. The beam is then photographed.

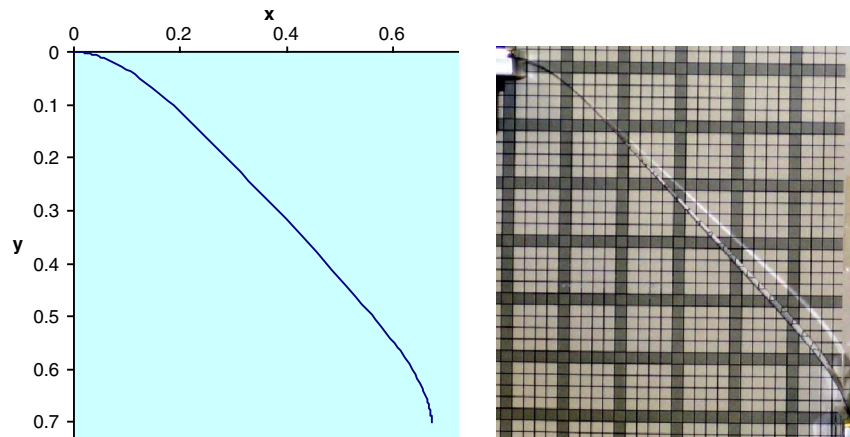


Fig. 3. The predicted shape versus the experimental shape in Case 1

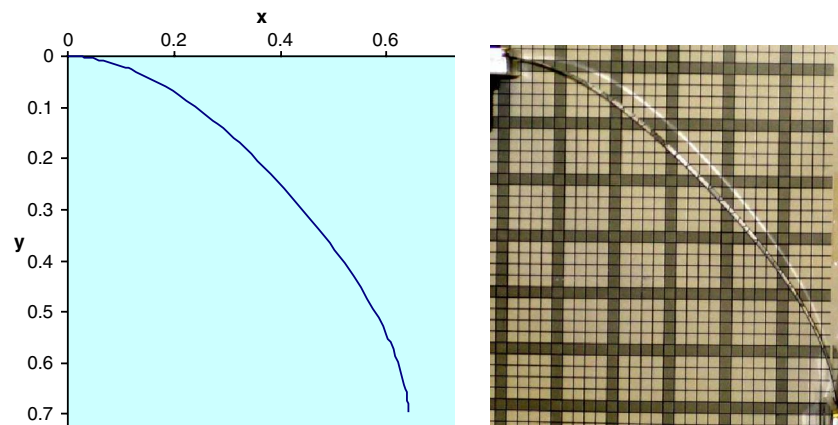


Fig. 4. The predicted shape versus the experimental shape in Case 2

Results

The experimental results for cases in which the curvature of the beam retains its sign over the length of the beam were compared numerically with solutions generated by solving Eqs. (7), (9), and (10). Table 1 lists the five cases studied and Figs. 3 to 7 present a comparison of the experimental and the predicted shapes. The coordinates of the free end of the beam are nondimensionalized against the beam length. In all cases, the predicted shape well matches the photographed shape. Cases 1 and 2 (Figs. 3 and 4, respectively) share a similar fastener location and orientation, but they differ in the length of the beam. The beam in Case 1 is shorter by approximately 6%. The net effect is that the beam is

“pulled tighter,” as Fig. 3 shows. The reaction forces are larger (see Table 1) and the beam shape is flatter in the central region.

To quantify the fit, five x -coordinate values were selected from each pair of corresponding beam shapes (numerical and experimental). Each x -coordinate identifies an interior point on the numerical and the experimental beam shapes, and consequently a distinct y -coordinate value for each shape. The absolute value of the difference in the y -coordinate between the numerical and experimental shapes (i.e., the absolute predictive error) is calculated for each point. The average absolute “% error,” which is nondimensionalized against beam length, was then calculated and tabulated in Table 1.

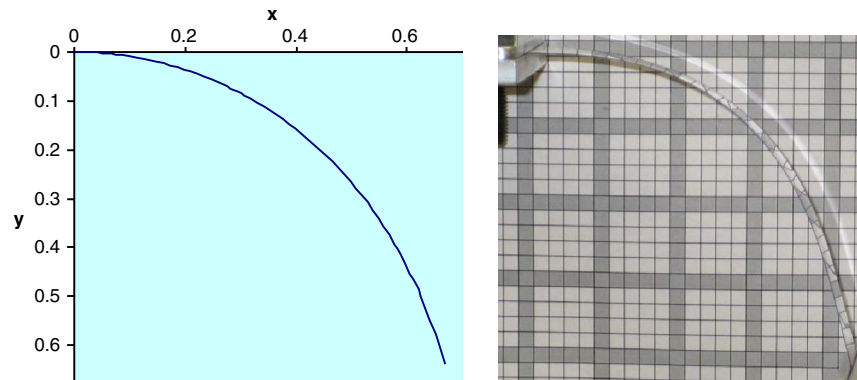


Fig. 5. The predicted shape versus the experimental shape in Case 3

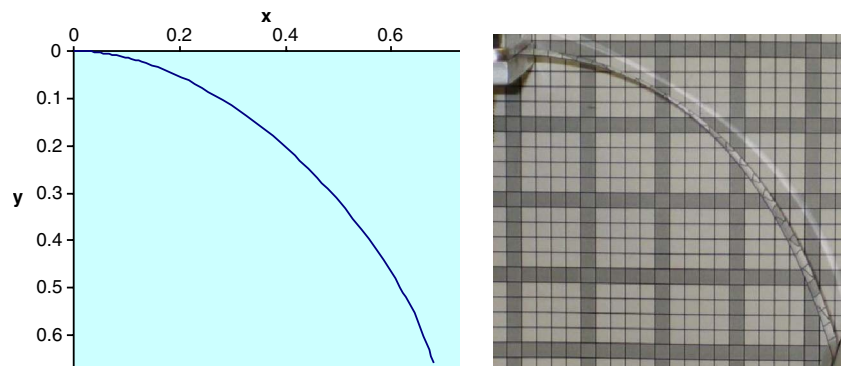


Fig. 6. The predicted shape versus the experimental shape in Case 4

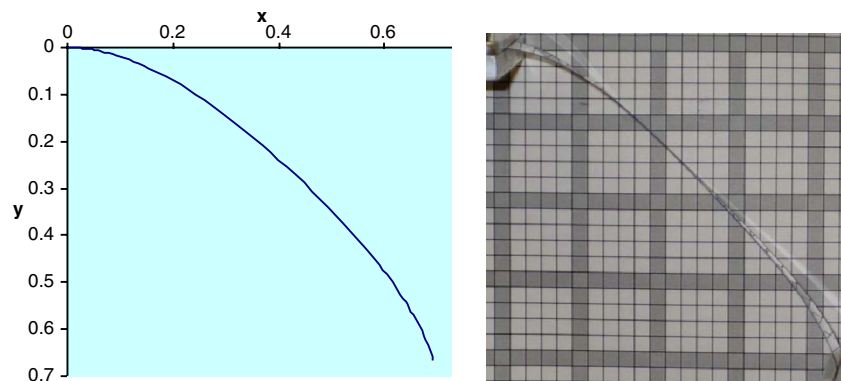


Fig. 7. The predicted shape versus the experimental shape in Case 5

Figs. 5 to 7 show that decreasing the length of the beam by a small amount while maintaining a similar fastener location and an identical orientation can result in a significant flattening of the draped shape in the mid region of the beam. The shapes in Figs. 5 to 7 in conjunction with the length column in Cases 3, 4, and 5 in Table 1 (218.4, 212.6, and 208.9 respectively) illustrate this. As the beam shape becomes flatter in the central region, the beam is pulled tighter and the reaction forces become progressively larger (see Table 1).

Conclusions

This paper has considered the special case of large deflection bending of a thin beam with no change in sign of the curvature. In particular, the authors of this paper have extended the analysis of Jairazbhoy et al. (2008). Photographs obtained from the experiments verified the numerical predictions. An excellent

agreement was found between the predicted and the photographed shapes.

References

- Cornil, M.-B., Capolungo, L., Qu, J., and Jairazbhoy, V. A. (2007). "Free vibration of a beam subjected to large static deflection." *J. Sound Vib.*, 303(3–5), 723–740.
- Freitag, L., et al. (2000). "Packaging aspects of the litebus parallel optoelectronic module." *Proc., 50th ECTC*, IEEE, Piscataway, NJ, 1259.
- Isaak, H., and Uka, P. (2000). "Development of flex stackable carriers." *Proc., 50th ECTC*, IEEE, Piscataway, NJ, 378.
- Jairazbhoy, V. A., Petukhov, P., and Qu, J. (2008). "Large deflection of thin plates in cylindrical bending—Non-unique solutions." *Int. J. Solids Struct.*, 45(11–12), 3203–3218.
- Xue, Y., Jairazbhoy, V. A., Niu, X., and Qu, J. (2003). "Large deflection of thin plates under certain mixed boundary conditions—Cylindrical bending." *J. Electron. Packag.*, 125(1), 53–58.